

Supporting Information

Evaluation of Process Severity on the Chemical Composition of Organosolv Switchgrass Lignins by Using Mass Spectrometry

Jifa Zhang,^a Yuan Jiang,^a Anton Astner,^b Hanyu Zhu,^a Joseph J. Bozell,^b and Hilikka I. Kenttämäa ^{a*}

^a Department of Chemistry, Purdue University, 560 Oval Drive, West Lafayette, Indiana 47907, United States

^b Center for Renewable Carbon, University of Tennessee, 2506 Jacob Drive, Knoxville, Tennessee 37996, United States

*Corresponding author: Hilikka I. Kenttämäa

E-mail: hilkka@purdue.edu

Table of Contents

Preparation of the organosolv switchgrass lignin samples	4
NMR data for sample S4	5
High-resolution mass spectra measured for the organosolv switchgrass samples by using (-)ESI HRMS.....	7
Figure S-1. High-resolution mass spectrum measured for the organosolv switchgrass sample S2 by using (-)ESI HRMS.	7
Figure S-2. High-resolution mass spectrum measured for the organosolv switchgrass sample S3 by using (-)ESI HRMS	7
Figure S-3. High-resolution mass spectrum measured for the organosolv switchgrass sample S5 by using (-)ESI HRMS	8
Figure S-4. High-resolution mass spectrum measured for the organosolv switchgrass sample S6 by using (-)ESI HRMS	8
High-resolution mass spectra measured for the organosolv switchgrass samples by using py/(-)APCI HRMS	9
Figure S-5. High-resolution mass spectrum measured for the organosolv switchgrass sample S1 by using py/(-)APCI HRMS.....	9
Figure S-6. High-resolution mass spectrum measured for the organosolv switchgrass sample S2 by using py/(-)APCI HRMS.....	10
Figure S-7. High-resolution mass spectrum measured for the organosolv switchgrass sample S3 by using py/(-)APCI HRMS.....	10
Figure S-8. High-resolution mass spectrum measured for the organosolv switchgrass sample S4 by using py/(-)APCI HRMS.....	11
Figure S-9. High-resolution mass spectrum measured for the organosolv switchgrass sample S5 by using py/(-)APCI HRMS.....	11
Figure S-10. High-resolution mass spectrum measured for the organosolv switchgrass sample S6 by using py/(-)APCI HRMS.....	12
Figure S-11. High-resolution mass spectrum measured for the organosolv switchgrass sample S7 by using py/(-)APCI HRMS.....	12
Table S1. HPLC retention times (R.T.) of the compounds detected in the organosolv switchgrass lignin sample S4, <i>m/z</i> values of the compounds deprotonated by (-)ESI and their determined elemental compositions as well as their RDBE values, their fragment ions and neutral fragments ^a formed upon CAD in MS ² to MS ⁴ experiments and their relative abundances, as well as the structure proposed for each neutral compound.	13
Structural elucidation of the common and abundant compounds in the organosolv lignin samples by using HPLC/(-)ESI HRMS ⁿ	16
High-resolution mass spectra measured for the organosolv switchgrass samples spiked with the internal standard by using (-)ESI HRMS. In the below spectra, ions of <i>m/z</i> 157 is the deprotonated internal standard ¹³ C ₆ -vanillin.....	18

Figure S-12. High-resolution mass spectrum measured for the organosolv switchgrass sample S1 spiked with the internal standard by using (-)ESI HRMS.....	18
Figure S-13. High-resolution mass spectrum measured for the organosolv switchgrass sample S2 spiked with the internal standard by using (-)ESI HRMS.....	19
Figure S-14. High-resolution mass spectrum measured for the organosolv switchgrass sample S3 spiked with the internal standard by using (-)ESI HRMS.....	19
Figure S-15. High-resolution mass spectrum measured for the organosolv switchgrass sample S4 spiked with the internal standard by using (-)ESI HRMS.....	20
Figure S-16. High-resolution mass spectrum measured for the organosolv switchgrass sample S5 spiked with the internal standard by using (-)ESI HRMS.....	20
Figure S-17. High-resolution mass spectrum measured for the organosolv switchgrass sample S6 spiked with the internal standard by using (-)ESI HRMS.....	21
Figure S-18. High-resolution mass spectrum measured for the organosolv switchgrass sample S7 spiked with the internal standard by using (-)ESI HRMS.....	22
References	22

Preparation of the organosolv switchgrass lignin samples

The preparation followed a previously published method.¹

Solvent Fractionation

Approximately 270 g of switchgrass (2.54-5.08 cm in length) was put into a perforated Teflon basket and placed in a flowthrough pressure reactor (Hastelloy C276). After sealing the flowthrough pressure reactor, it was placed under vacuum for a time of 30 min. A solution of water, ethanol, and methyl isobutyl ketone (MIBK) (50/34/16 wt %) in the presence of H₂SO₄ (at a concentration of 0.025, 0.05, or 0.1M) was added into the flowthrough pressure reactor under vacuum. The mixture was heated to a fractionation temperature of 120, 140, or 160 °C. The fractionation was run for a time of 56 or 120 min. The additional solvent was pumped into a collection tank through the system during the time of fractionation to generate approximately 3.5 – 4.5 L of black solution. After the fractionation was completed, the solvent remaining in the flowthrough pressure reactor was transferred into the collection tank carefully. After cooling down, the reactor was opened and the undissolved cellulose in the Teflon basket was removed.

Lignin recovery

Method 1

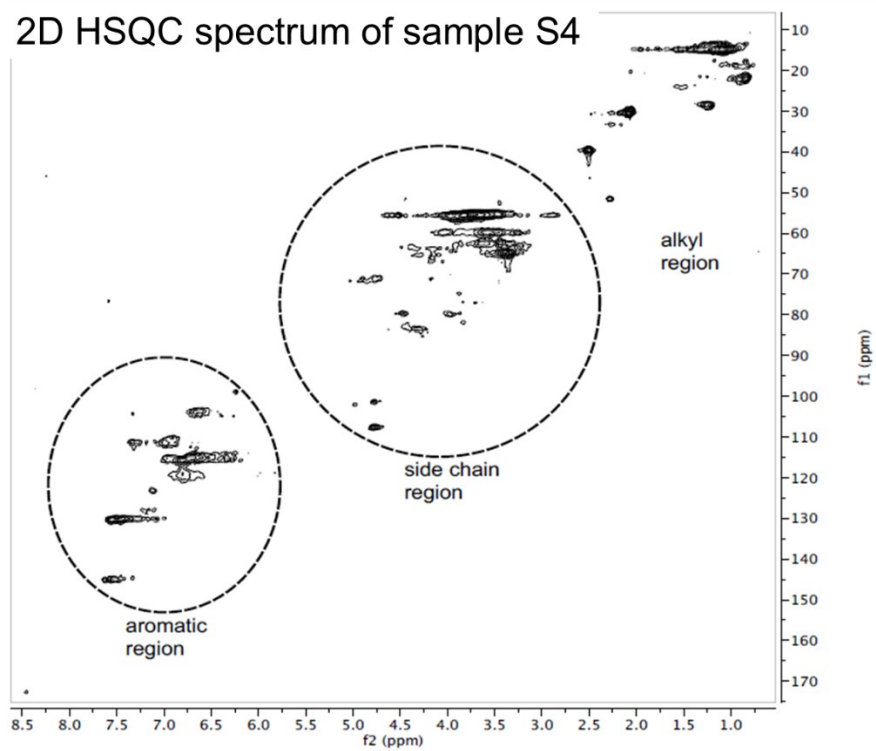
The black liquor in the collection tank was mixed with 25% v/v deionized water in a separatory funnel. The funnel was shaken to mix the mixture well and then the mixture was allowed to stand for 30 min. An aqueous and organic phase was formed. After removing the aqueous phase, the organic phase was filtered through Celite in a Büchner funnel. The filtered organic phase was concentrated via rotatory evaporation to afford crude lignin. The afforded crude lignin was triturated with diethyl ether. Then diethyl ether was decanted. The triturated lignin was placed under vacuum overnight. The trituration step was repeated as necessary to give a free-flowing brown organosolv lignin powder.

Method 2

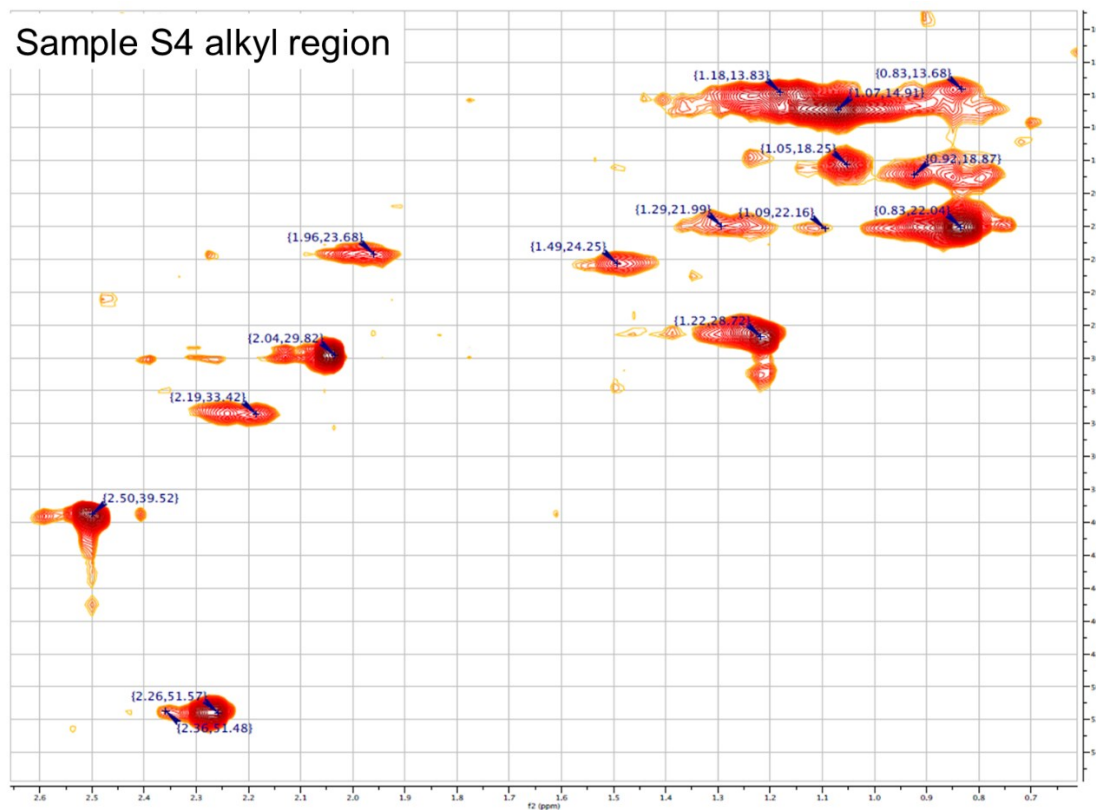
To resulted black liquor in a separatory funnel, solid NaCl (10 g per 100 mL water contained in the solvent mixture) was added. Then the separatory funnel was shaken and was allowed to stand for 30 min. An aqueous phase and an organic phase were formed. The organic phase was washed with ~50% v/v water and ~75% v/v water. The organic fraction was concentrated via rotatory evaporation to afford crude lignin. The afforded crude lignin was triturated with diethyl ether. After decanting the diethyl ether, the remaining lignin was placed under vacuum. The trituration step was repeated as necessary to give a free-flowing brown organosolv lignin powder.

NMR data for sample S4

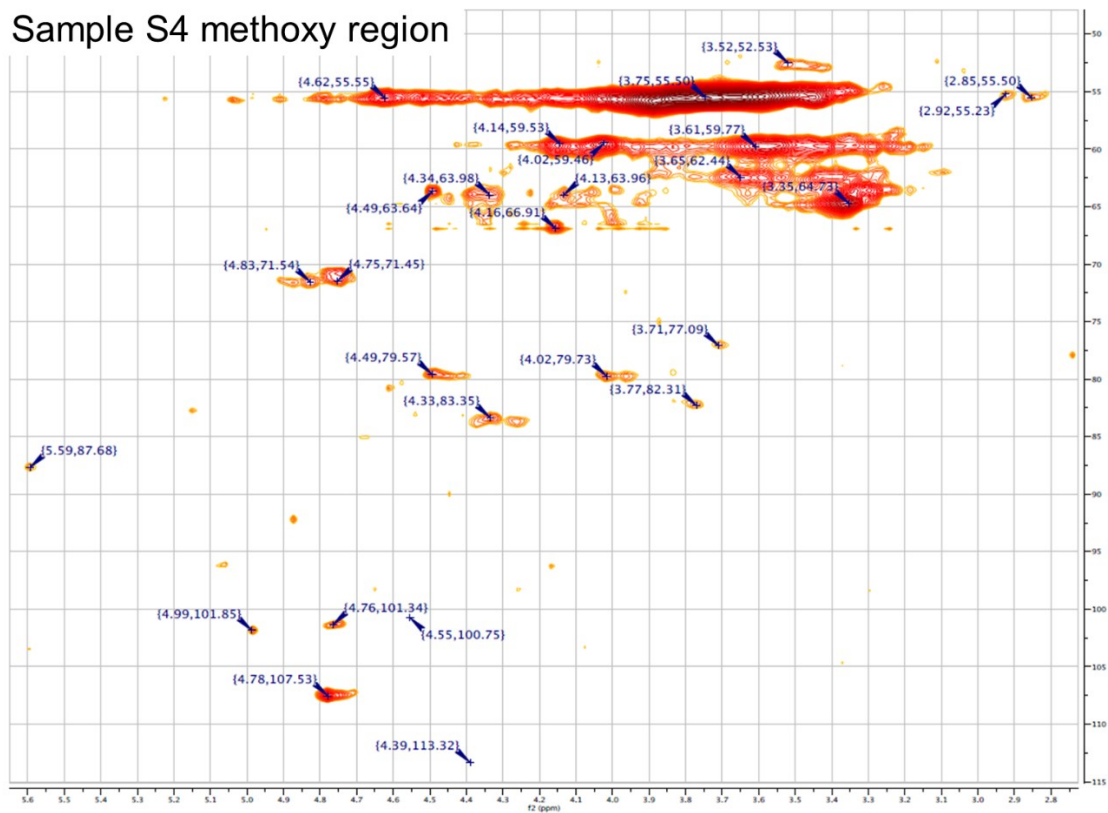
2D HSQC spectrum of sample S4



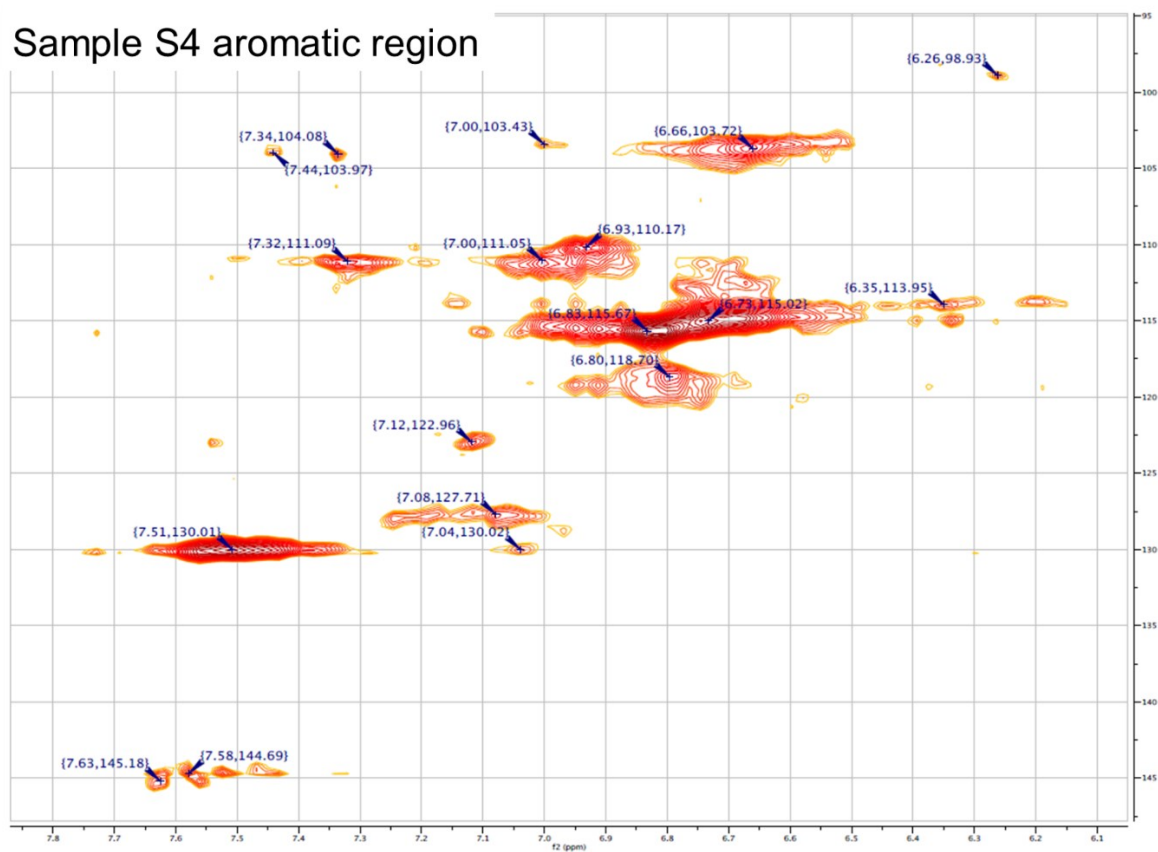
Sample S4 alkyl region



Sample S4 methoxy region



Sample S4 aromatic region



High-resolution mass spectra measured for the organosolv switchgrass samples by using (-)ESI HRMS

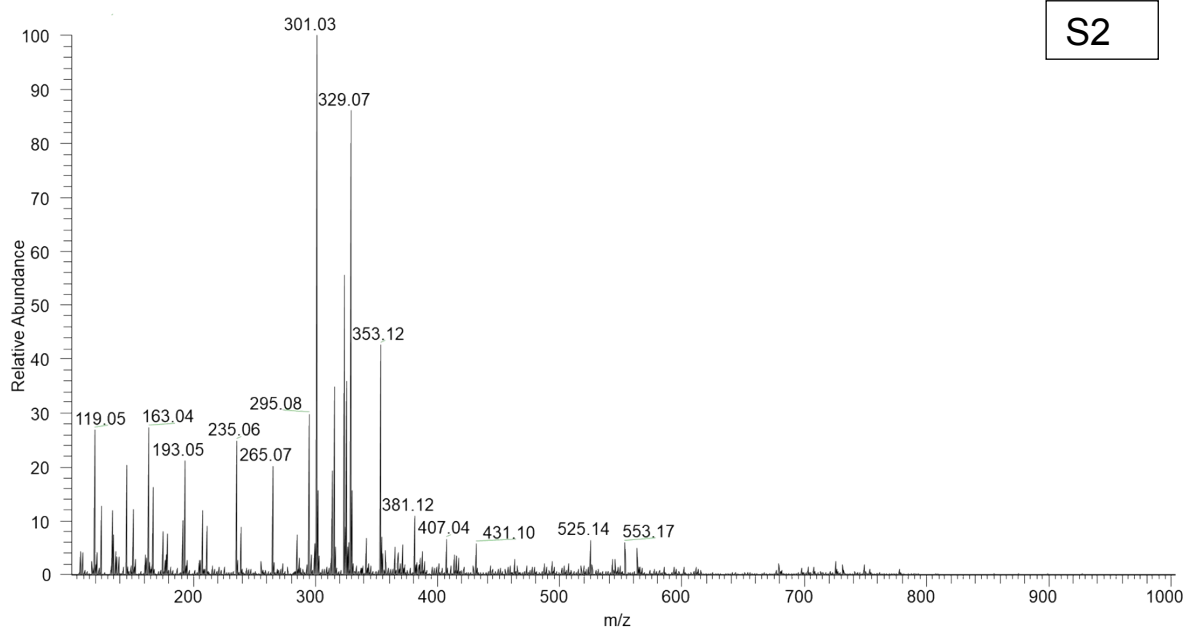


Figure S-1. High-resolution mass spectrum measured for the organosolv switchgrass sample **S2** by using (-)ESI HRMS.

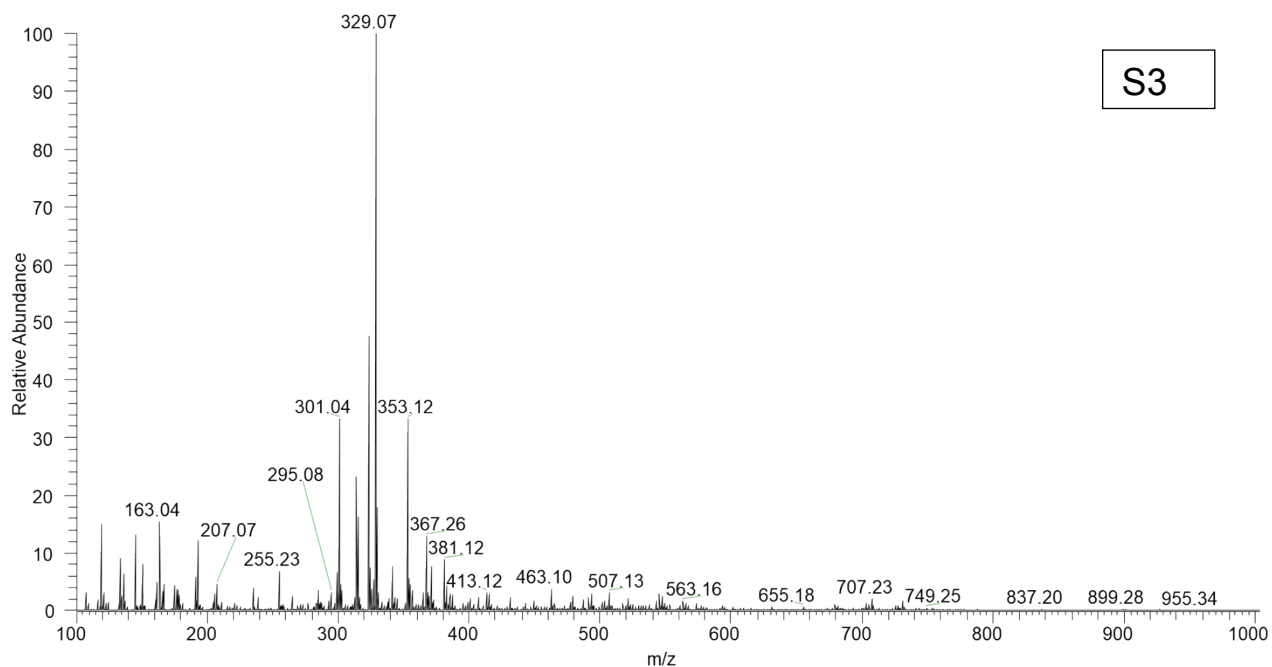


Figure S-2. High-resolution mass spectrum measured for the organosolv switchgrass sample **S3** by using (-)ESI HRMS

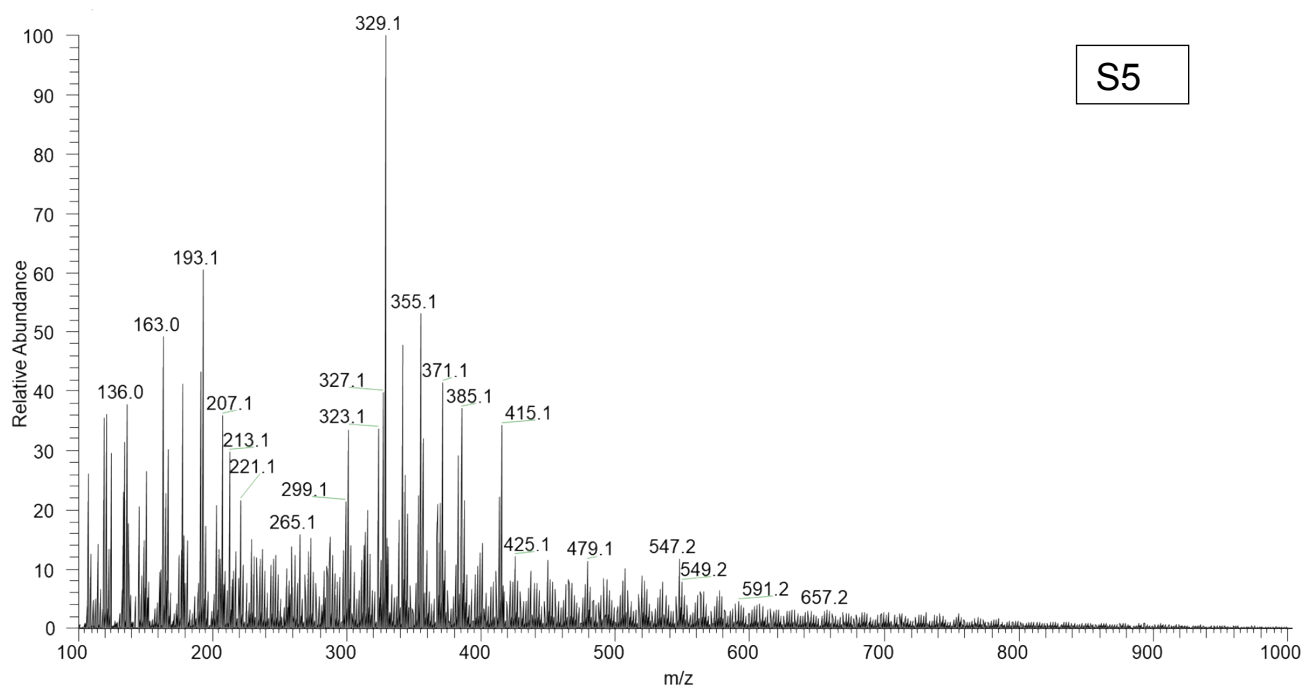


Figure S-3. High-resolution mass spectrum measured for the organosolv switchgrass sample **S5** by using (-)ESI HRMS

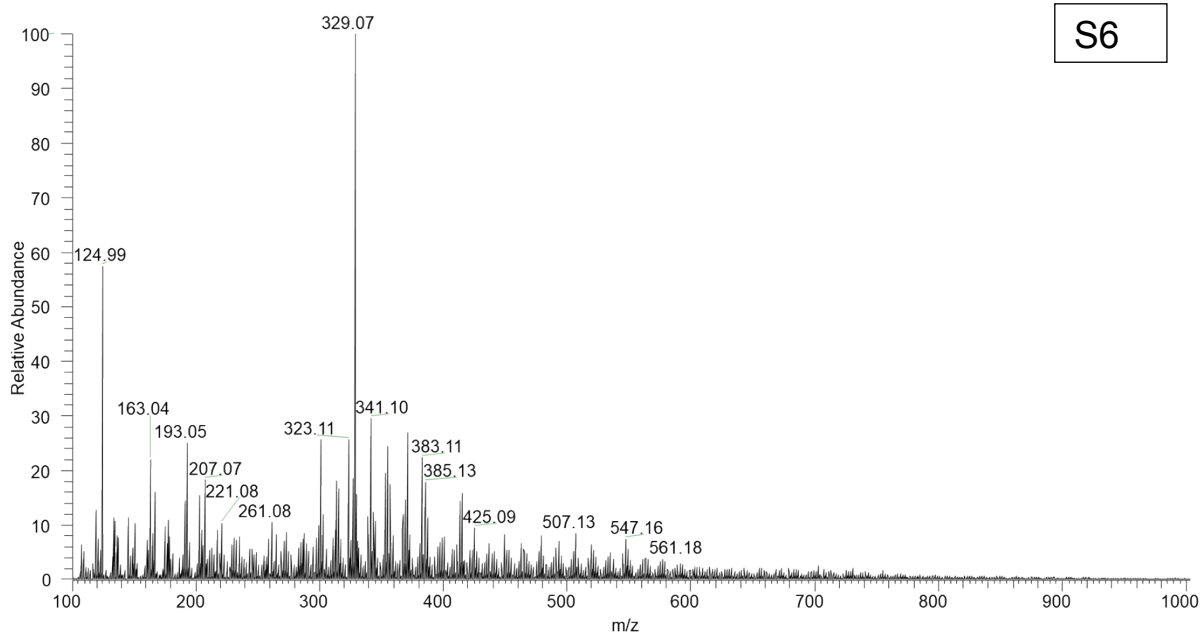
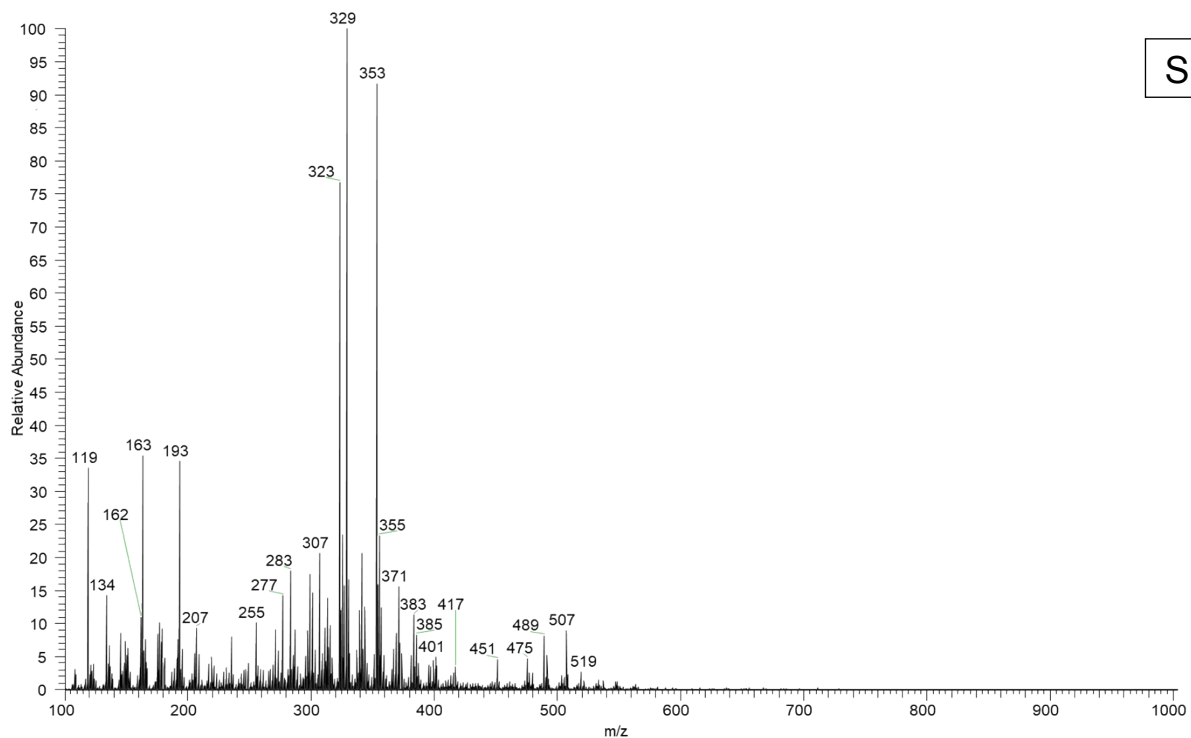


Figure S-4. High-resolution mass spectrum measured for the organosolv switchgrass sample **S6** by using (-)ESI HRMS

High-resolution mass spectra measured for the organosolv switchgrass samples by using py/(-)APCI HRMS



S1

Figure S-5. High-resolution mass spectrum measured for the organosolv switchgrass sample S1 by using py/(-)APCI HRMS.

S2

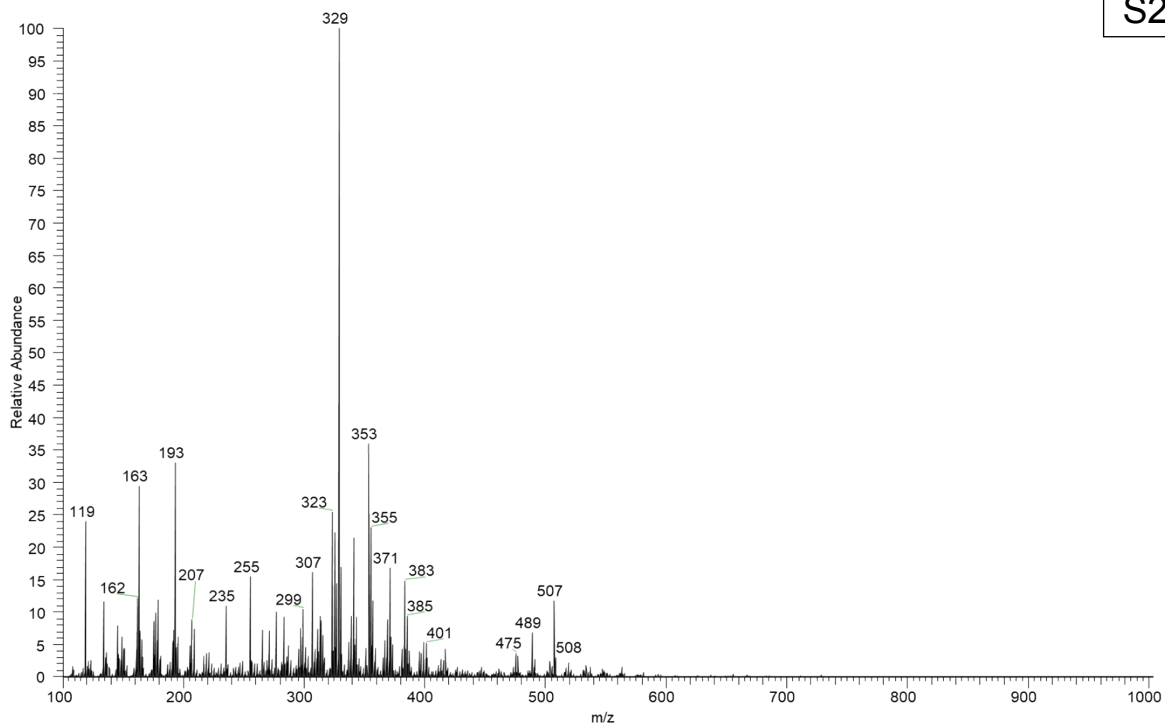


Figure S-6. High-resolution mass spectrum measured for the organosolv switchgrass sample **S2** by using py/(-)APCI HRMS.

S3

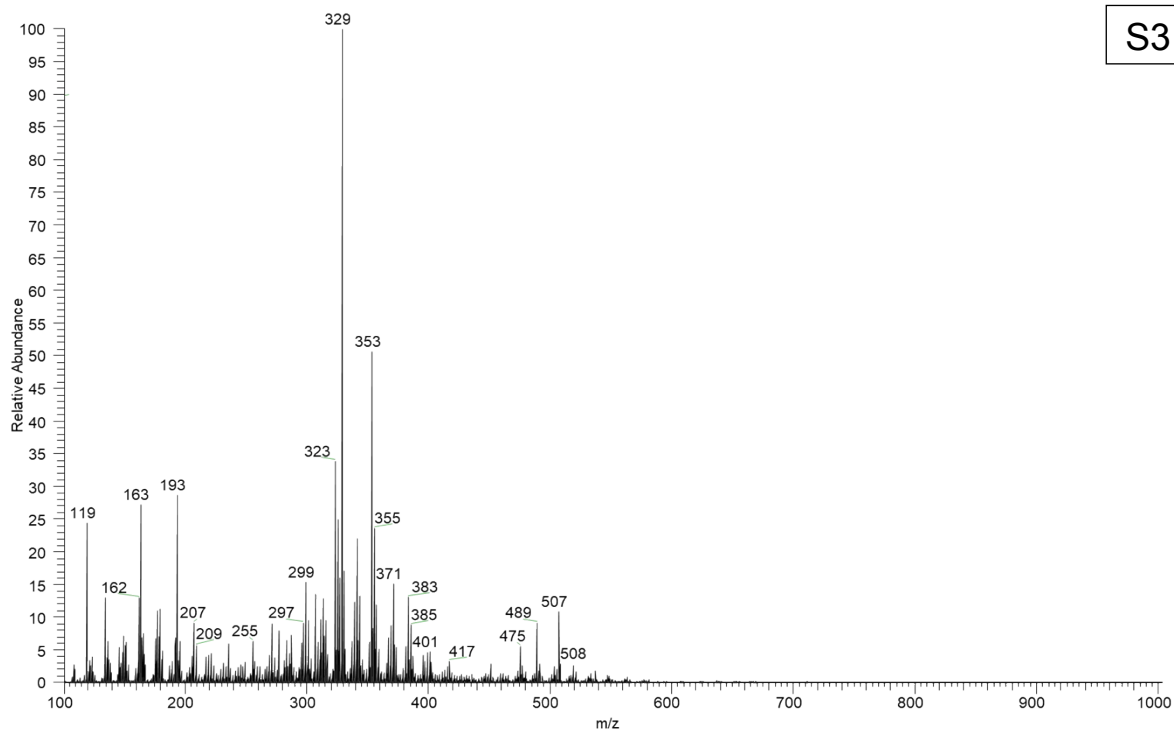


Figure S-7. High-resolution mass spectrum measured for the organosolv switchgrass sample **S3** by using py/(-)APCI HRMS.

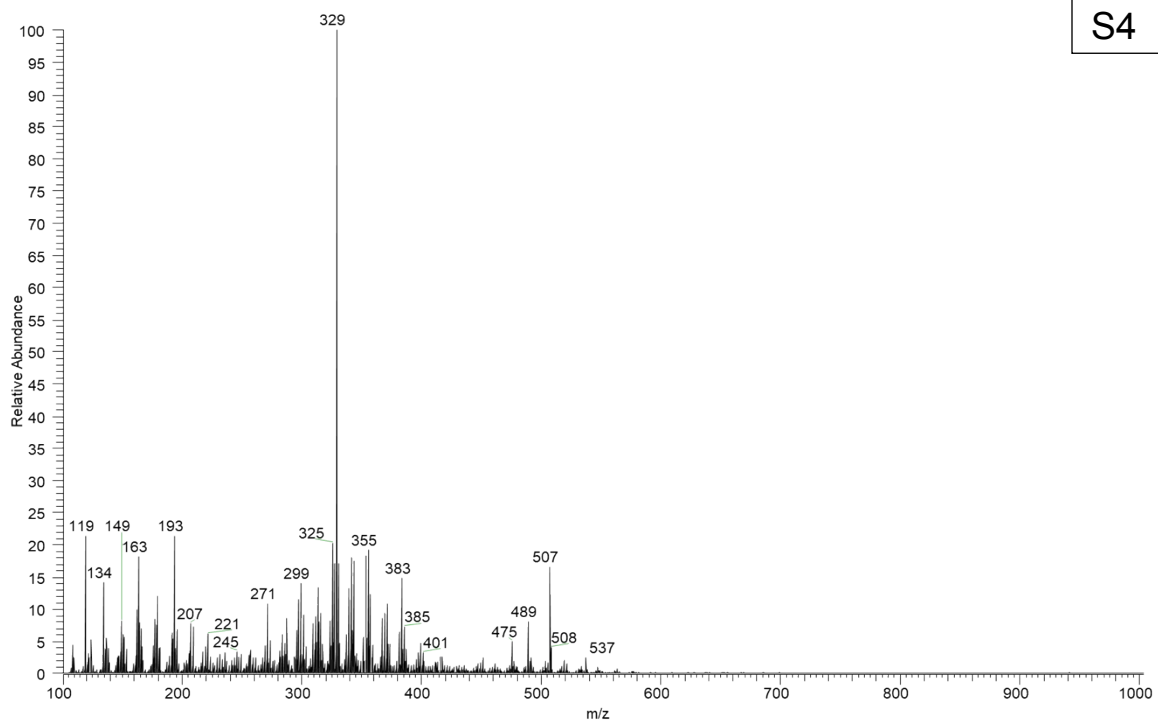


Figure S-8. High-resolution mass spectrum measured for the organosolv switchgrass sample **S4** by using py/(-)APCI HRMS.

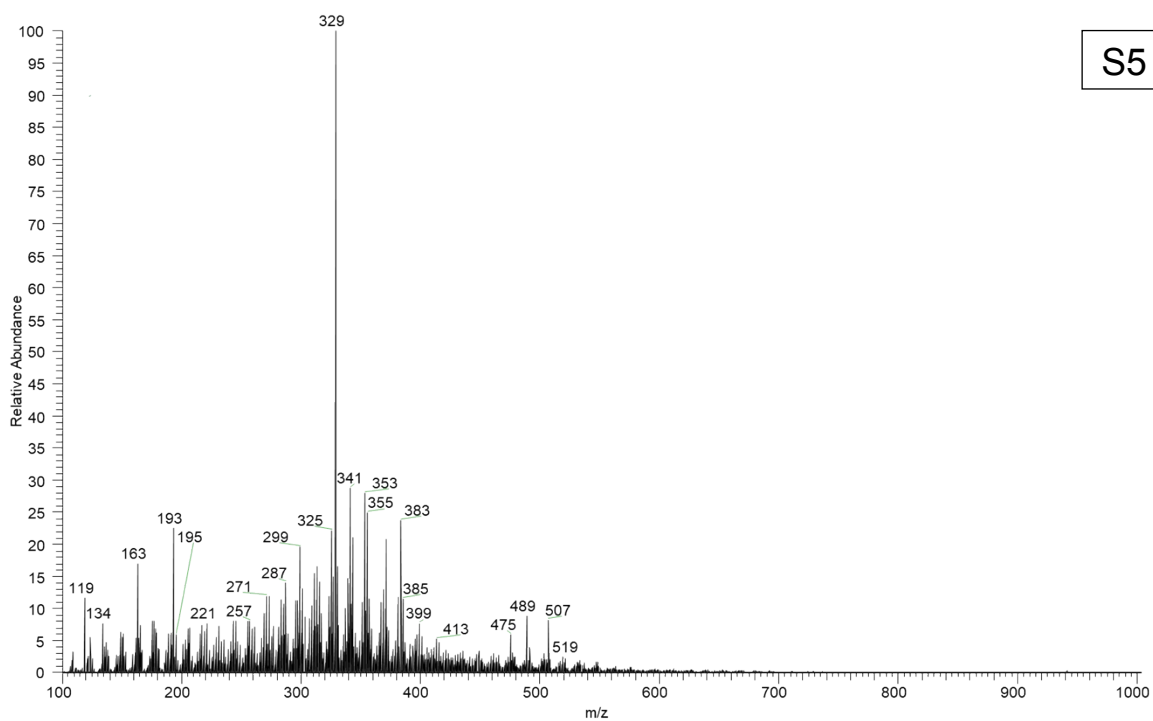
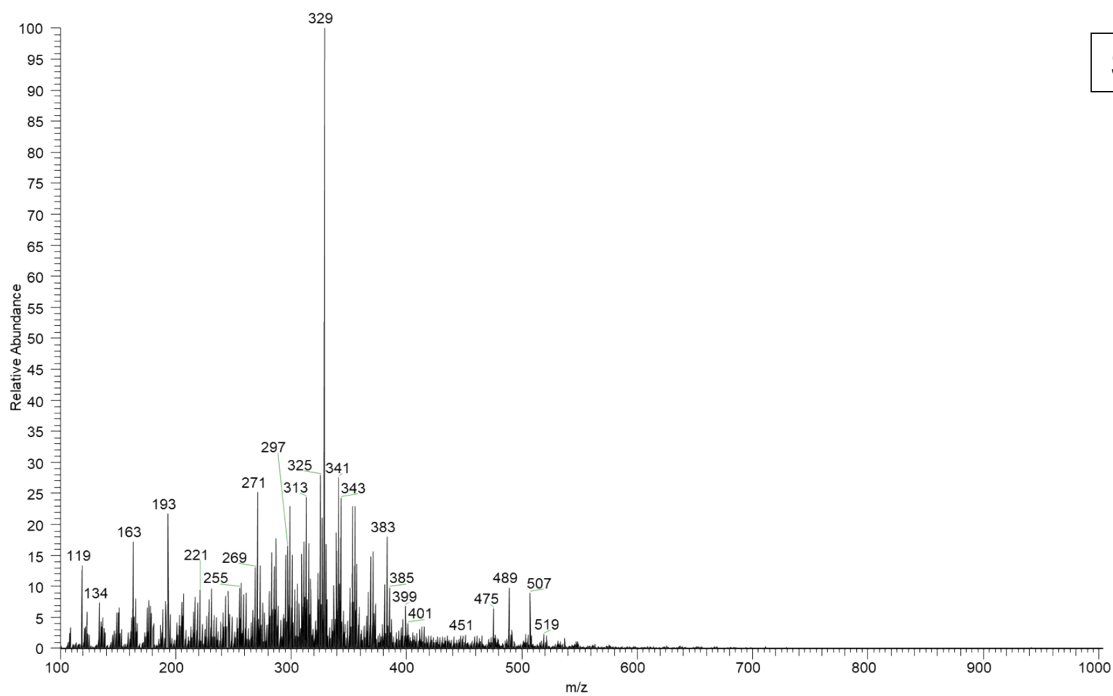
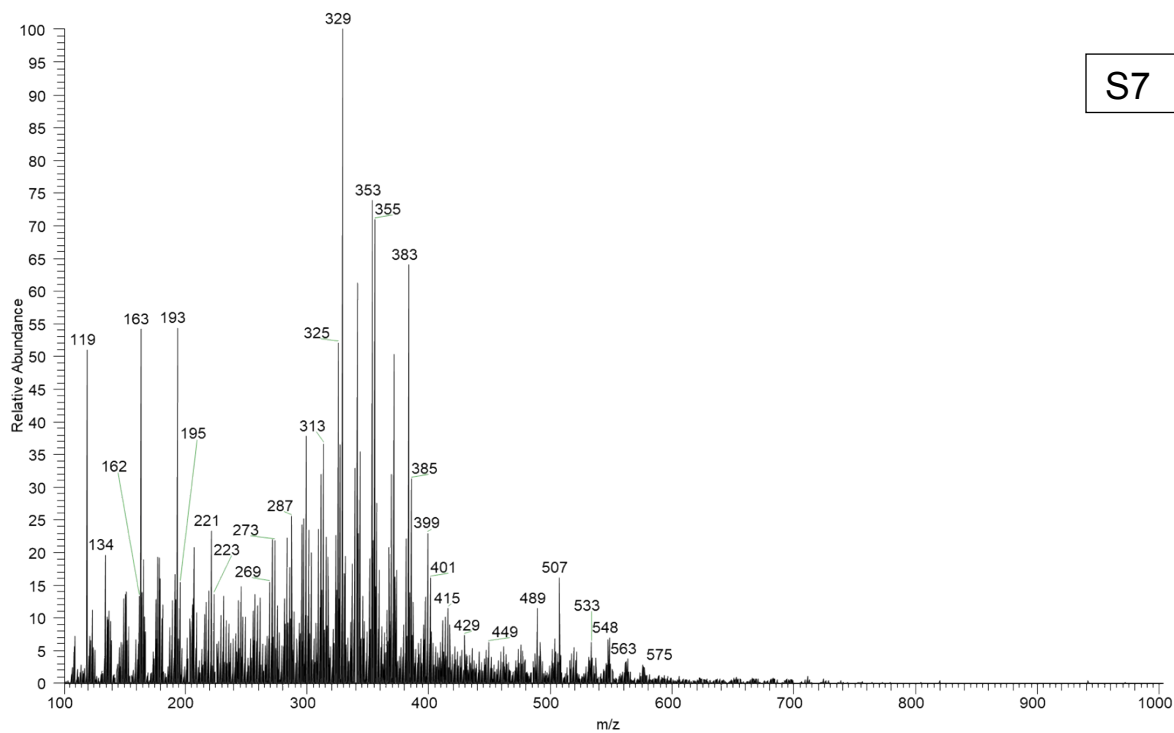


Figure S-9. High-resolution mass spectrum measured for the organosolv switchgrass sample **S5** by using py/(-)APCI HRMS.



S6

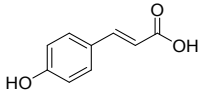
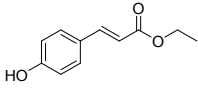
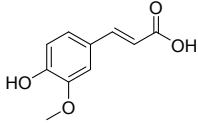
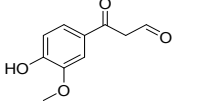
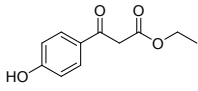
Figure S-10. High-resolution mass spectrum measured for the organosolv switchgrass sample S6 by using py/(-)APCI HRMS.

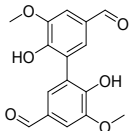


S7

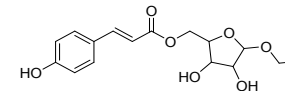
Figure S-11. High-resolution mass spectrum measured for the organosolv switchgrass sample S7 by using py/(-)APCI HRMS.

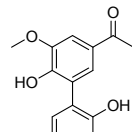
Table S1. HPLC retention times (R.T.) of the compounds detected in the organosolv switchgrass lignin sample S4, *m/z* values of the compounds deprotonated by (-)ESI and their determined elemental compositions as well as their RDBE values, their fragment ions and neutral fragments^a formed upon CAD in MS² to MS⁴ experiments and their relative abundances, as well as the structure proposed for each neutral compound.

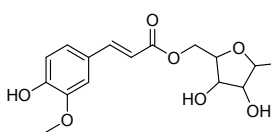
R.T. (min)	<i>m/z</i>	Elemental composition	RDBE	MS ²	MS ³	MS ⁴	Proposed structure
7.8	163^b	C ₉ H ₇ O ₃	6.5	163-CO ₂ (119) 100%			
18.9	191^b	C ₁₁ H ₁₁ O ₃	6.5	191-C ₂ H ₄ (163) 100% 191-C ₂ H ₅ OH (145) 30% 191-C ₂ H ₄ -CO ₂ (119) 26%	163-CO ₂ (119) 100%		
8.6	193^b	C ₁₀ H ₉ O ₄	6.5	193-CO ₂ (149) 100% 193-•CH ₃ (178) 95% 193-CO ₂ -•CH ₃ (134) 58%	149-•CH ₃ (134) 100%		
13.3	193	C ₁₀ H ₉ O ₄	6.5	193-•CH ₃ (178) 100%	178-CH ₂ CO (136) 100% 178-CO (150) 10% 178-CH ₂ CO-CO (108) 5%	136-CO (108) 100%	
14.6	207	C ₁₁ H ₁₁ O ₄	6.5	207-C ₂ H ₄ (179) 100% 207-C ₂ H ₄ -CO ₂ (135) 21% 207-C ₂ H ₅ OH (161) 19%	179-CO ₂ (135) 100%		

				207-•C ₂ H ₅ -CO ₂ (134) 10%			
				207-•C ₂ H ₅ (179) 3%			
16.4	301^b	C ₁₆ H ₁₃ O ₆	10.5	301-•CH ₃ (286) 100%	286-H ₂ O (268) 100%	268-CO (240) 100%	
				301-•CH ₃ -CO (258) 50%	286-•CHO (257) 90%	268-•CHO (239) 20%	
					286-H ₂ O-CO (240) 55%	268-2CO (212) 10%	
					286-•OH (269) 50%		
					286-H ₂ O - H• (267) 40%		
					286-H ₂ O-•CHO (239) 35%		
					286-CO-•CHO (229) 15%		
					286-•CH ₃ (271) 10%		

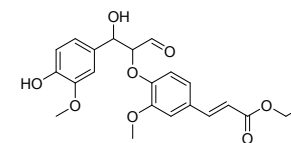
9.9	323	C ₁₆ H ₁₉ O ₇	7.5	323-C ₇ H ₁₂ O ₄ (163) 100%	163-CO ₂ (119) 100%	
				323-C ₇ H ₁₄ O ₅ (145) 90%		
				323- C ₇ H ₁₂ O ₄ -CO ₂ (119) 30%		
				323-C ₂ H ₅ OH (277) 8%		
				323- C ₇ H ₁₄ O ₅ -CO (117) 6%		



18.2	329	C ₁₇ H ₁₃ O ₇	11.5	329-•CH ₃ (314) 100%	314-•CH ₃ (299) 100%	299-CO (271) 100%	
					314-•CHO (285) 10%	299-CO-CO ₂ (227) 20%	

10.9	353	C ₁₇ H ₂₁ O ₈	7.5	353-C ₇ H ₁₄ O ₅ (175) 100%	175-•CH ₃ (160) 100%	160-CO (132) 100%	
------	------------	--	-----	--	---------------------------------	-------------------	---

				353-C ₇ H ₁₄ O ₅ -•CH ₃ (160) 30%		
				353-•CH ₃ (338) 25%		
				353-C ₇ H ₁₂ O ₄ (193) 15%		
15.3	415	C ₂₂ H ₂₃ O ₈	11.5	415-C ₁₀ H ₁₀ O ₄ (221) 100%	221-•CH ₃ (206) 100%	206-•C ₂ H ₅ (177) 100%
				415-C ₂ H ₅ OH-CO ₂ (325) 65%		206-•C ₂ H ₅ -CO ₂ (133) 55%
				415-C ₂ H ₅ OH-CO ₂ -•CH ₃ (310) 65%		
				415-C ₁₀ H ₁₀ O ₄ -•CH ₃ (206) 50%		
				415-C ₁₂ H ₁₄ O ₄ (193) 40%		
				415-C ₂ H ₅ OH-CO ₂ -CO (297) 35%		



^aThe elemental compositions of the fragmenting and the fragment ions were determined. The elemental compositions of the eliminated neutral molecules were derived from the elemental compositions of the fragmenting ions and the fragment ions. The fragment ions are shown in descending order of relative abundances. The information in the MS² to MS⁴ columns is shown in the following order: *m/z* of the precursor ion, the elemental composition of the neutral fragment lost upon CAD, *m/z* of the product ion (in parenthesis), and the relative abundance of the fragment ion. The reproducibility of the relative abundances of the fragment ions was $\pm 15\%$.

^bThese structures were verified by comparing the observed fragmentation patterns to those of deprotonated authentic model compounds or to data published previously on deprotonated authentic model compounds.²

Structural elucidation of the common and abundant compounds in the organosolv lignin samples by using HPLC/(-)ESI HRMSⁿ

The structures of ions of m/z 163, ions of m/z 191, one ionic isomer of m/z 193, and ions of m/z 301 were confirmed by comparing their fragmentation patterns with those of the deprotonated model compounds. This is already mentioned in the manuscript, thus only the other ions are discussed here.

Monomeric ions

Isomeric ions of m/z 193 fragmented by losing a $\bullet\text{CH}_3$ upon CAD in an MS² experiment, indicating a methoxy group exists in the ions of m/z 193. A molecule of $\text{CH}_2=\text{C}=\text{O}$ was eliminated upon CAD in an MS³ experiment, and a CO molecule was eliminated upon further CAD in an MS⁴ experiment. Based on the elemental composition and the fragmentation pattern, the isomeric ions of m/z 193 are identified as deprotonated 3-(4-hydroxy-3-methoxyphenyl)-3-oxopropanal (Table S1).

Ions of m/z 207 eliminated C_2H_4 , both C_2H_4 and CO_2 , $\text{C}_2\text{H}_5\text{OH}$, both $\bullet\text{C}_2\text{H}_5$ and CO_2 , and $\bullet\text{C}_2\text{H}_5$ in an MS² experiment. The elimination of $\text{C}_2\text{H}_5\text{OH}$ indicates that the unknown ion contains an ethyl ester functionality.² No elimination of $\bullet\text{CH}_3$ from ions of m/z 207 was observed, indicating that no methoxy groups are present in these ions. Considering the elemental composition and the fragmentation pattern of the ions of m/z 207, they are proposed to correspond to a deprotonated β -ketoester (Table S1).

Lignin-carbohydrate complexes

Two major ions of m/z 323 and 353 were identified as deprotonated *p*-coumarate and ferulate carbohydrate esters, respectively. Upon CAD, the ions of m/z 323 generate fragment ions of m/z 163 via the loss of a neutral molecule with the formula $\text{C}_7\text{H}_{12}\text{O}_4$ (Table S1). The fragment ions of m/z 163 fragment by losing a CO_2 molecule. The fragmentation of the fragment ions of m/z 163 matches that reported for deprotonated *p*-coumaric acid,² thus confirming its structure. Upon CAD, the ions of m/z 323 also form fragment ions of m/z 145 via the elimination of a neutral molecule with the formula $\text{C}_7\text{H}_{14}\text{O}_5$. The low C/O ratio (C/O ratio = 1.4) and low RDBE value of the lost neutral molecule ($\text{C}_7\text{H}_{14}\text{O}_5$, RDBE = 1) indicate that the lost neutral molecule likely corresponds to a carbohydrate.^{3,4} Therefore, ions of m/z 323 are assigned to correspond to a *p*-coumaroylated-carbohydrate complex. On the other hand, the ions of m/z 353 eliminated a neutral molecule with the elemental composition $\text{C}_7\text{H}_{14}\text{O}_5$ upon CAD. Similarly, this neutral molecule is likely to correspond to a carbohydrate due to its low C/O ratio and low RDBE value.^{3,4} Elimination of a neutral molecule with the elemental composition $\text{C}_7\text{H}_{12}\text{O}_5$ was also observed to generate ions of m/z 193. These ions have a low abundance and further CAD experiments were not performed as the automated HPLC/(-)ESI HRMSⁿ experiments only isolated the most abundant ion for CAD experiments in each stage. Based on the proposed structures, ions of m/z 353 belong to the deprotonated feruloylated-carbohydrate complex class.

Lignin dimer with a β -O-4 linkage

A compound with a β -O-4 linkage (corresponding to ions of m/z 415) was detected in the organosolv lignin mixture studied. The CAD patterns of deprotonated oligomeric lignin β -O-4 model compounds have been identified to involve three major pathways (Scheme 1A):⁵ elimination of the charge-remote unit(s) B; elimination of the charged end unit A; and elimination of water and formaldehyde from the side chain. Cleavage of the β -O-4 linkage is involved in both the elimination of the charge-remote unit(s) and the charged end unit A upon CAD.⁵⁻⁷ Observance of fragment ions derived from the above pathways upon CAD of a deprotonated compound implies that the compound contains a β -O-4 linkage. Upon CAD of the ions of m/z 415, ions of m/z 193 and 221 were generated via the elimination of neutral molecules of MW of 222 and 194 Da, respectively. This fragmentation matches that published for deprotonated oligomeric lignin model compounds with β -O-4 linkages (Scheme 1A).⁵ If the ions of m/z 415 contain a β -O-4 linkage, ions of m/z 193 (ions A) would be generated via the elimination of a neutral molecule of MW 222 Da (molecule B), and ions of m/z 221 (ions B) would be generated via the

elimination of a neutral molecule of MW 194 Da (molecule A). Therefore, ions of m/z 415 are concluded to contain a β -O-4 linkage. The proposed pathways for the generation of the two major fragment ions of m/z 193 and 221 upon CAD of ions of m/z 415 are shown in Scheme 1B. When the ions of m/z 221 (generated in the MS² experiment) were isolated and subjected to CAD, they fragmented by losing a $\bullet\text{CH}_3$ in an MS³ experiment and by losing $\bullet\text{C}_2\text{H}_5$ and both $\bullet\text{C}_2\text{H}_5$ and CO_2 in an MS⁴ experiment. The fragmentations of the fragment ions of m/z 221 match those of deprotonated ethyl ferulate,² indicating that the unknown fragment ions of m/z 221 correspond to deprotonated ethyl ferulate. The structure proposed for the ions of m/z 415 and the pathways proposed for the formation of their major fragment ions of m/z 193 and 221 are shown in Scheme 1B.

Lignin dimer with a 5-5 linkage

Ion of m/z 329 contains a 5-5 linkage. Ions of m/z 329 lost two $\bullet\text{CH}_3$ upon CAD, indicating that two methoxy groups existed in the ions of m/z 329. Loss of $\bullet\text{CHO}$ upon CAD indicates the existence of a formaldehyde functionality.^{2,4} Based on all these findings, a structure was proposed for the deprotonated compounds of m/z 329 with a 5-5 linkage (Table S1).

High-resolution mass spectra measured for the organosolv switchgrass samples spiked with the internal standard by using (-)ESI HRMS. In the below spectra, ions of m/z 157 is the deprotonated internal standard $^{13}\text{C}_6$ -vanillin

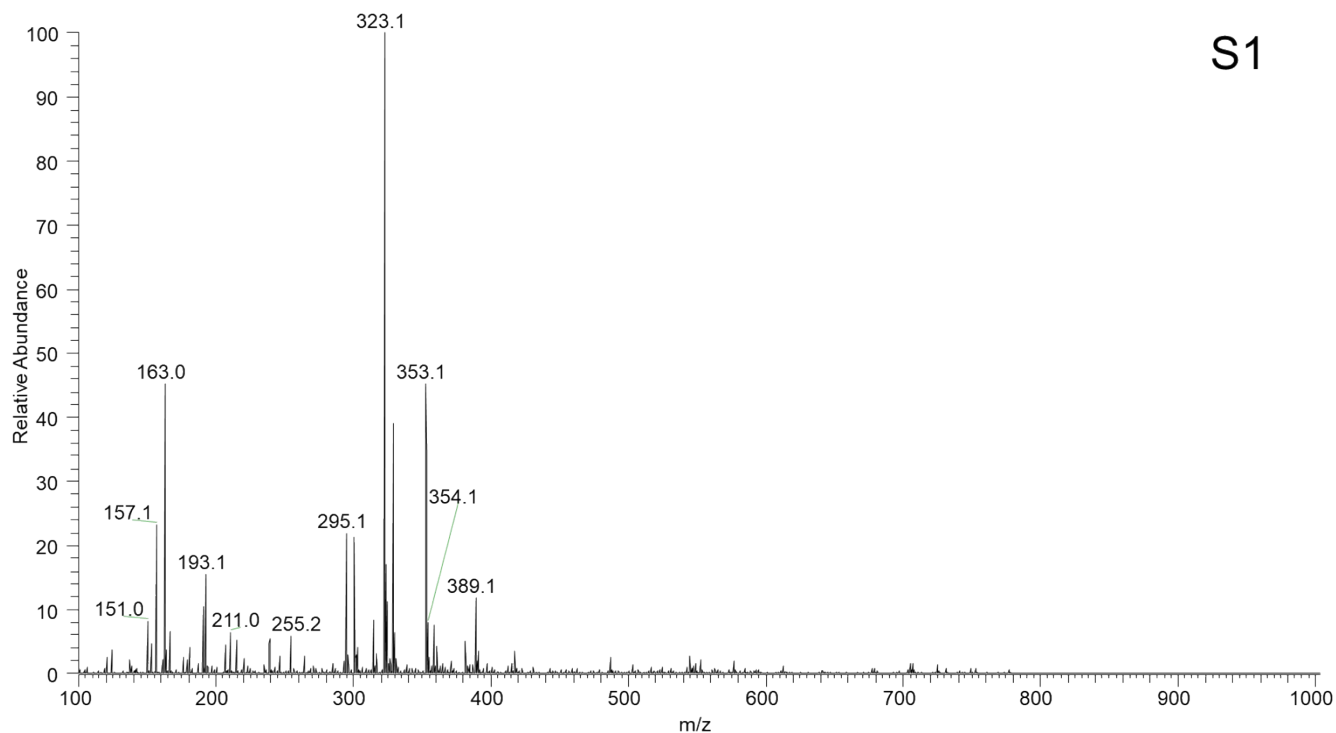


Figure S-12. High-resolution mass spectrum measured for the organosolv switchgrass sample **S1** spiked with the internal standard by using (-)ESI HRMS.

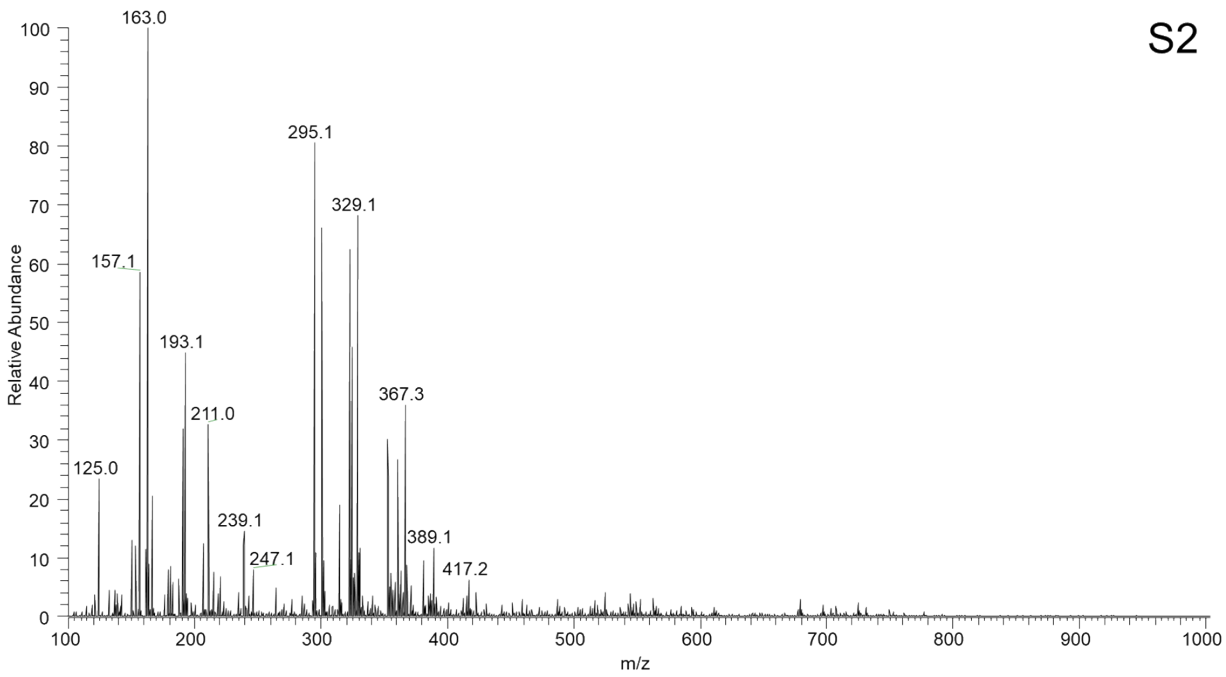


Figure S-13. High-resolution mass spectrum measured for the organosolv switchgrass sample **S2** spiked with the internal standard by using (-)ESI HRMS.

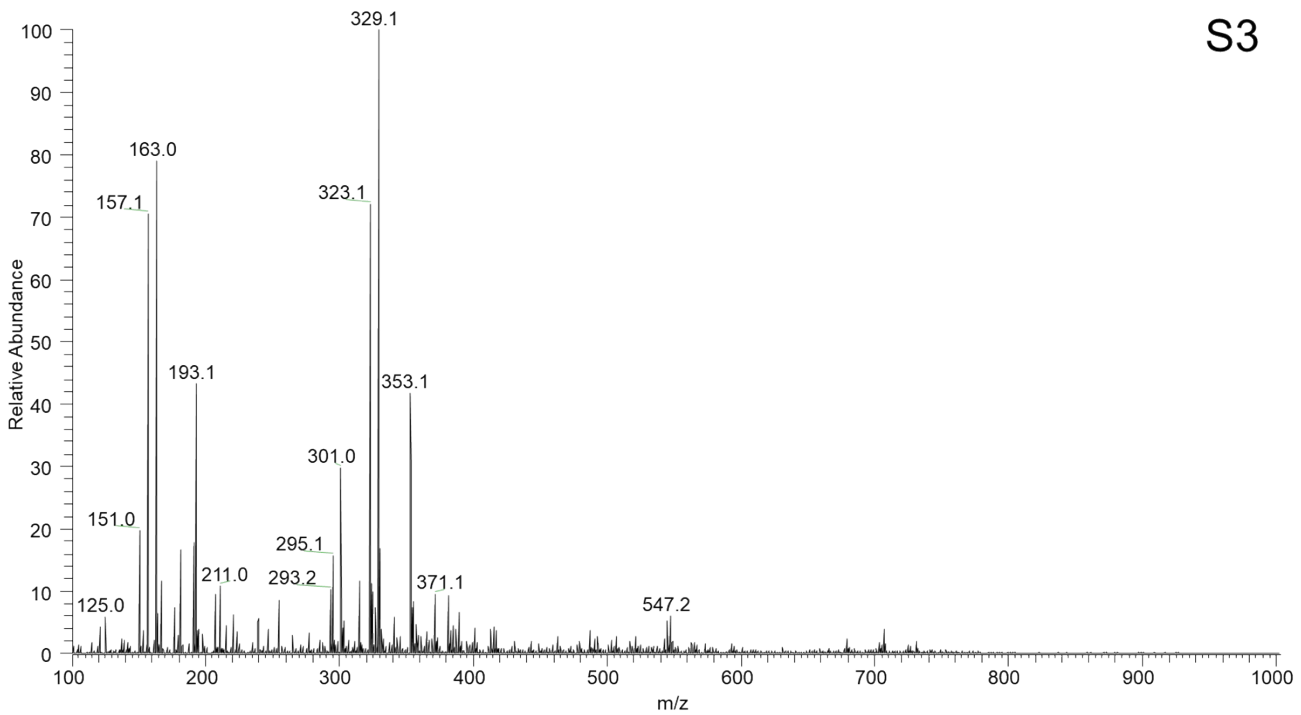


Figure S-14. High-resolution mass spectrum measured for the organosolv switchgrass sample **S3** spiked with the internal standard by using (-)ESI HRMS.

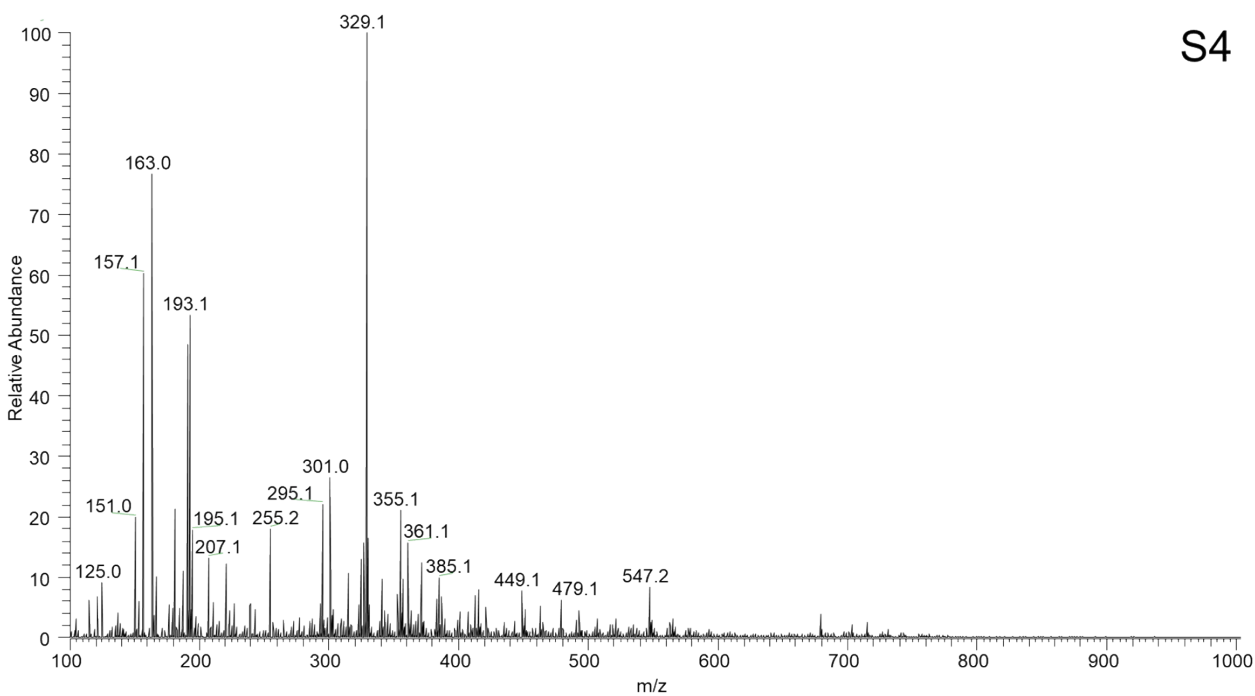


Figure S-15. High-resolution mass spectrum measured for the organosolv switchgrass sample **S4** spiked with the internal standard by using (-)ESI HRMS.

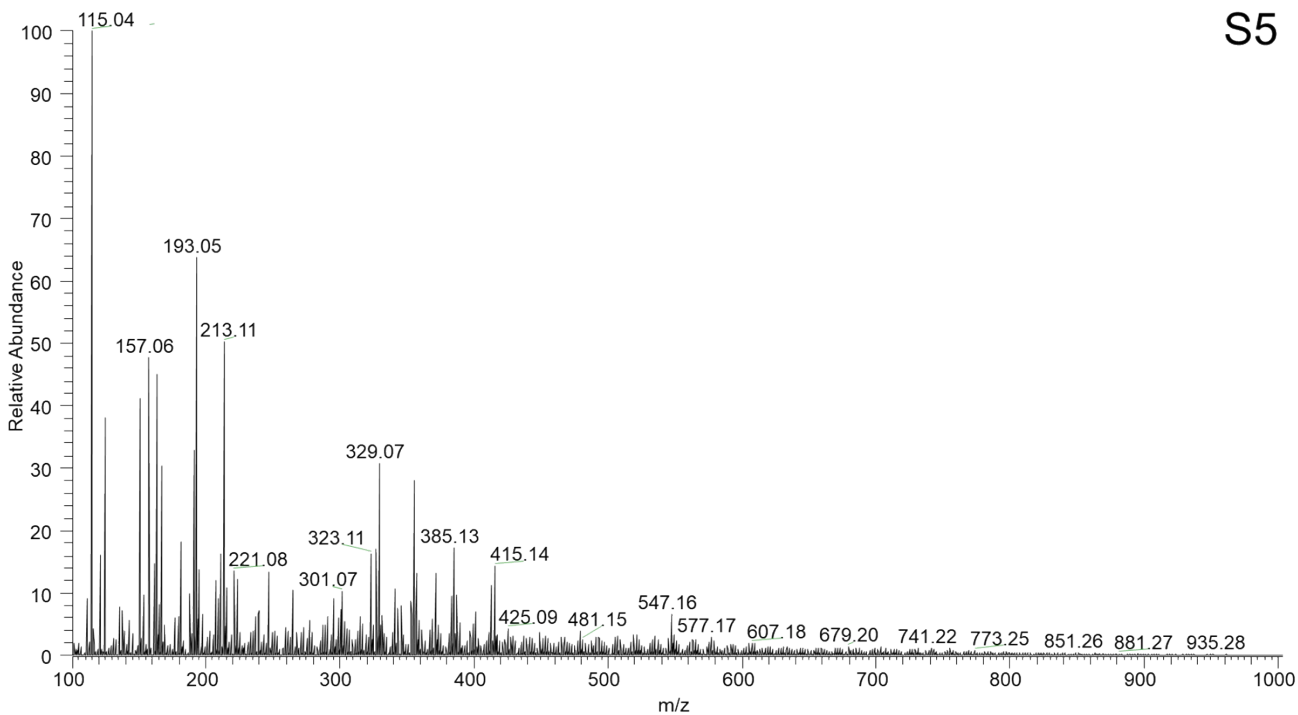


Figure S-16. High-resolution mass spectrum measured for the organosolv switchgrass sample **S5** spiked with the internal standard by using (-)ESI HRMS.

S6

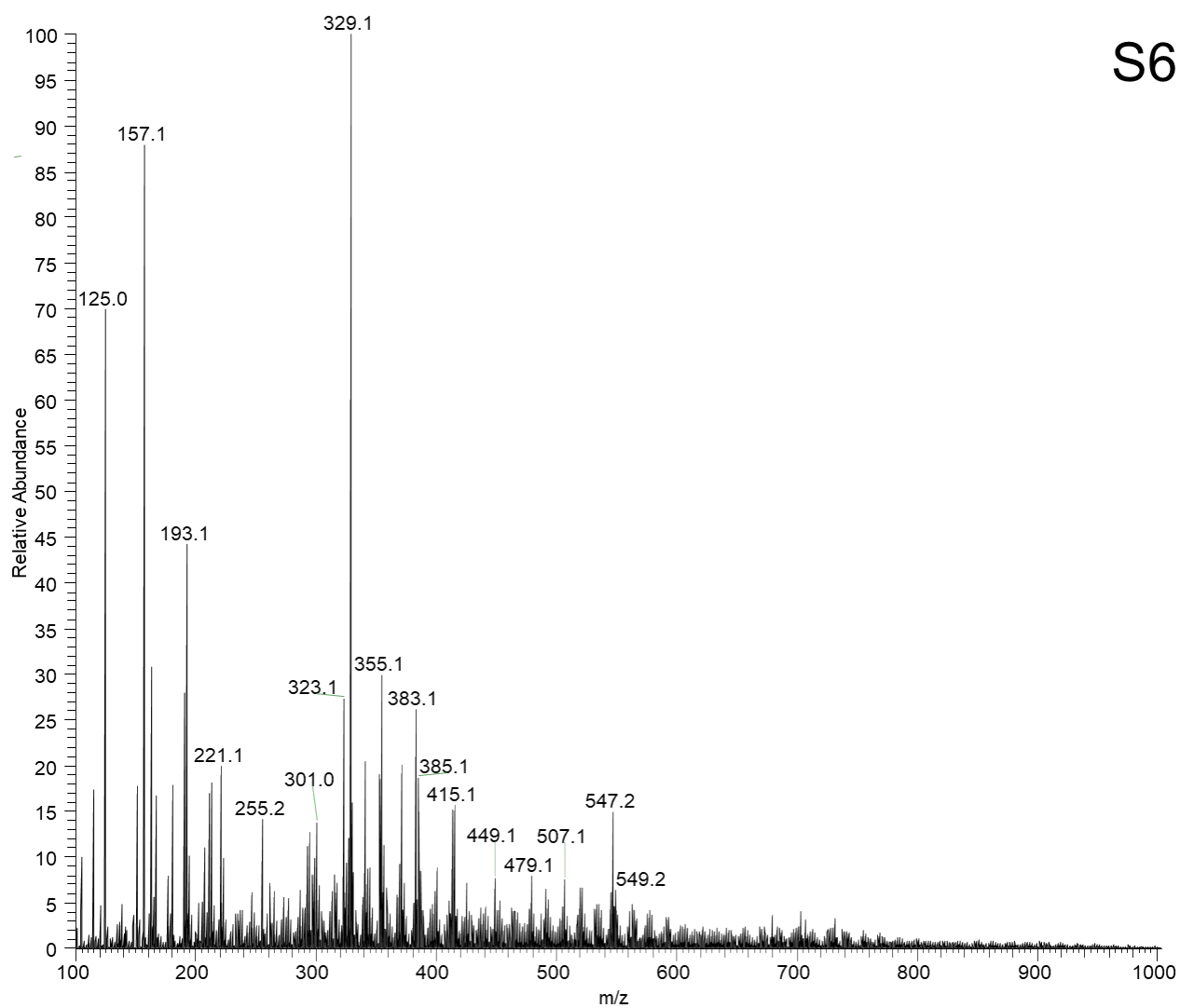


Figure S-17. High-resolution mass spectrum measured for the organosolv switchgrass sample **S6** spiked with the internal standard by using (-)ESI HRMS.

S7

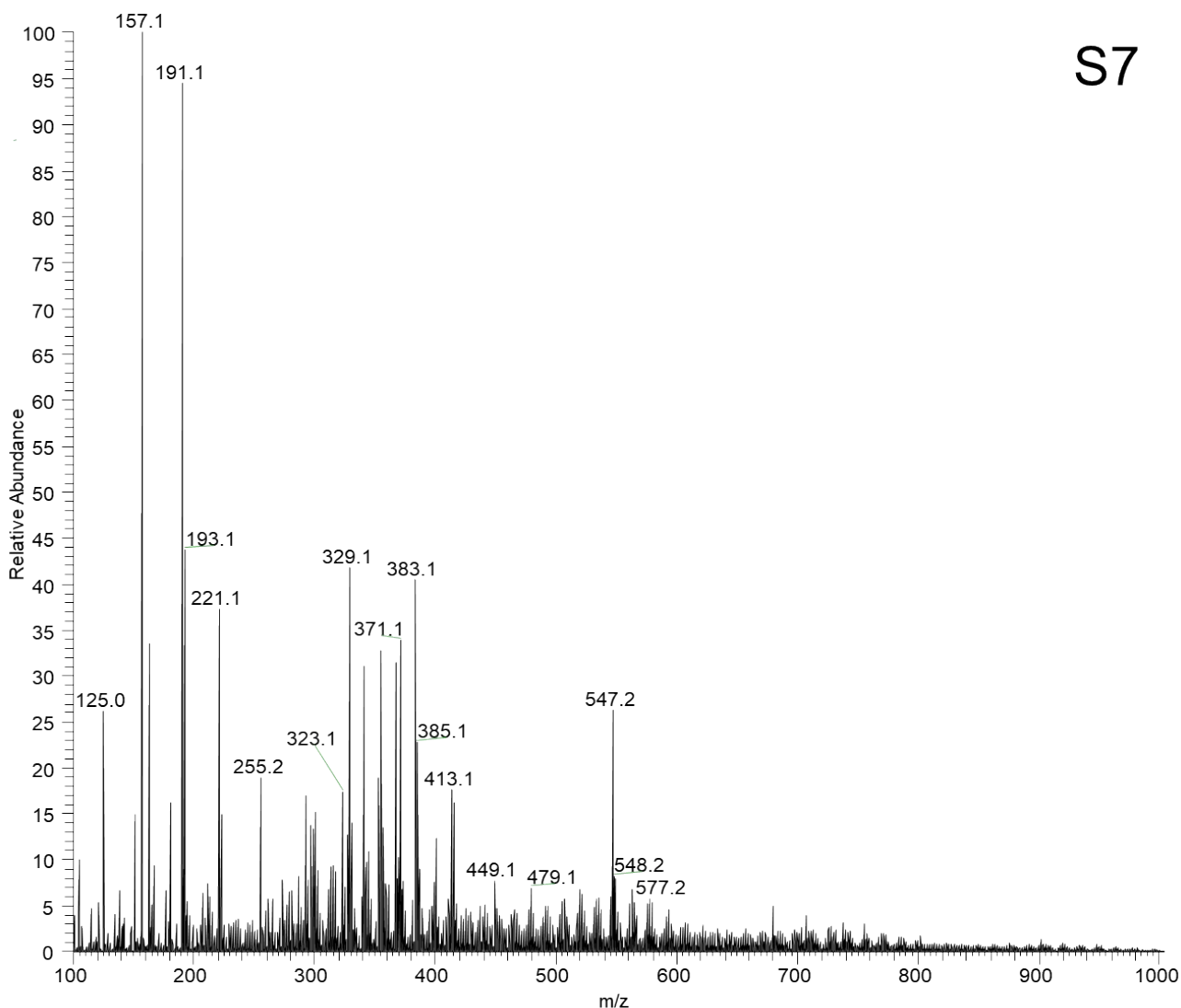


Figure S-18. High-resolution mass spectrum measured for the organosolv switchgrass sample S7 spiked with the internal standard by using (-)ESI HRMS.

References

1. Bozell, J. J.; O'Lenick, C. J.; Warwick, S., Biomass fractionation for the biorefinery: heteronuclear multiple quantum coherence-nuclear magnetic resonance investigation of lignin isolated from solvent fractionation of switchgrass. *J. Agric. Food Chem.* **2011**, *59* (17), 9232-9242.
2. Marcum, C. L.; Jarrell, T. M.; Zhu, H.; Owen, B. C.; Hauptert, L. J.; Easton, M.; Hosseinaei, O.; Bozell, J.; Nash, J. J.; Kenttämä, H. I., A fundamental tandem mass spectrometry study of the collision-activated dissociation of small deprotonated molecules related to lignin. *ChemSusChem* **2016**, *9* (24), 3513-3526.
3. Jarrell, T. M.; Marcum, C. L.; Sheng, H.; Owen, B. C.; O'Lenick, C. J.; Maraun, H.; Bozell, J. J.; Kenttämä, H. I., Characterization of organosolv switchgrass lignin by using high performance liquid chromatography/high resolution tandem mass spectrometry using hydroxide-doped negative-ion mode electrospray ionization. *Green Chem.* **2014**, *16* (5), 2713-2727.

4. Zhang, J.; Jiang, Y.; Easterling, L. F.; Anton, A.; Li, W.; Alzarini, K. A.; Dong, X.; Bozell, J.; Kenttämä, H. K., Compositional analysis of organosolv poplar lignin by using high-performance liquid chromatography/high-resolution multi-stage tandem mass spectrometry. *Green Chem.* **2021**, *23* (2), 983-1000.
5. Zhang, J.; Feng, E.; Li, W.; Sheng, H.; Milton, J. R.; Easterling, L. F.; Nash, J. J.; Kenttämä, H. I., Studies on the fragmentation mechanisms of deprotonated lignin model compounds in tandem mass spectrometry. *Anal. Chem.* **2020**, *92* (17), 11895–11903.
6. Morreel, K.; Kim, H.; Lu, F. C.; Dima, O.; Akiyama, T.; Vanholme, R.; Niculaes, C.; Goeminne, G.; Inze, D.; Messens, E.; Ralph, J.; Boerjan, W., Mass spectrometry-based fragmentation as an identification tool in lignomics. *Anal. Chem.* **2010**, *82* (19), 8095-8105.
7. Sheng, H.; Tang, W.; Gao, J.; Riedeman, J. S.; Li, G.; Jarrell, T. M.; Hurt, M. R.; Yang, L.; Murria, P.; Ma, X.; Nash, J. J.; Kenttämä, H. I., (-)ESI/MSⁿ procedure for sequencing lignin oligomers based on a study of synthetic model compounds with β -O-4 and 5-5 linkages. *Anal. Chem.* **2017**, *89* (24), 13089-13096.